



## **Adaptive mesh refinement strategy for the phase field method using variable-node finite element**

Gihwan Kim<sup>1)</sup> \*Phill-Seung Lee<sup>2)</sup>

*<sup>1),2)</sup> Department of Mechanical Engineering, Korea Advanced Institute of Science and Technology, Daehak-ro 291, Yuseong-gu, Daejeon 34141, Korea*

*\* Corresponding author. Tel: +82 42 350 1512; E-mail address: phillseung@kaist.edu*

### **ABSTRACT**

The phase field method has attracted the attention of academia in recent a decade due to the advantage of being able to handle topologically complex fractures such as branching cracks and initiation. However, in order to ensure the accuracy of the simulation, mesh refinement at the vicinity of the crack tip is necessary. Various adaptive mesh refinement strategies for the phase field method have been proposed, but those are not easy to use due to the cumbersome of modeling. In this study, we present an adaptive mesh refinement strategy for the phase field method to simulate brittle fracture problems. The h-refined mesh is used around the crack tip and the coarse mesh is used away from the crack tip. The fine mesh and the coarse mesh are connected in a simple way using variable-node finite element. The fine mesh where the crack tip passed is changed into the coarse mesh for computational efficiency. The performance of the strategy is shown through two-dimensional crack numerical examples. In the future, we will extend this study by applying numerical techniques such as the strain smoothing method and the enriched finite element. Also, it is valuable to extend this study to shell fracture.

### **1. INTRODUCTION**

Fracture is a very important phenomenon in that it can cause catastrophic accidents in humanity. In order to prevent these accidents, understanding the fracture behavior is essential. Several theories have been proposed to understand the fracture behavior from the engineering point of view (Inglis 1913, Griffith 1921). In addition, there have been many attempts to simulate the fracture behavior through numerical methods, some of which have been very successful (Belytschko 1999, Silling 2000).

Recently, the phase field method that can easily handle topologically complex fractures such as crack initiation or crack branching was proposed (Miehe et. al. 2010) and has attracted the attention of academia. However, mesh refinement at the vicinity of

---

<sup>1)</sup> Ph.D. Student

<sup>2)</sup> Professor



the crack tip is required to ensure the simulation accuracy. Several researchers have presented adaptive mesh refinement strategies for the phase field method (Patil et. al. 2018, Tian et. al. 2019), which are not easy to use due to the difficulty of modeling.

In this study, an adaptive mesh refinement strategy for the phase field method to simulate brittle fracture problems is presented. The fine mesh around the crack tip and the coarse mesh far from the crack tip are connected in a simple way using variable-node finite elements (Lim et. al. 2012).

In the following sections, we briefly review the formulation of the phase field method, and its performance is presented.

## 2. Formulation

### 2.1. Phase field approximation

An elastic continuous body  $\Omega$  containing an internal sharp crack surface  $\Gamma$  is considered as shown in Fig. 1a.  $\partial\Omega_N$  and  $\partial\Omega_D$  represents the Neumann and Dirichlet boundaries, respectively.

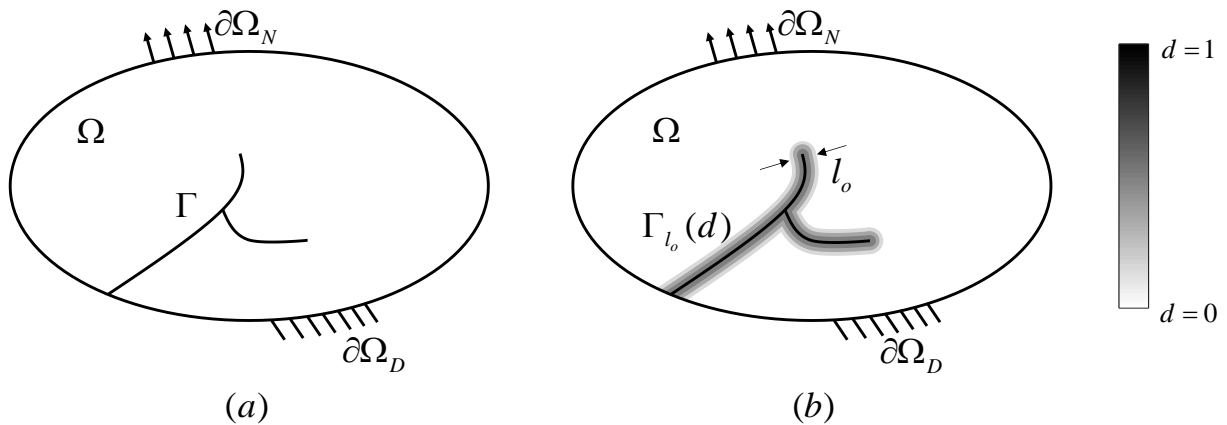


Fig. 1 Schematic of a solid body  $\Omega$  (a) with a sharp crack surface  $\Gamma$ , (b) with a diffuse crack surface  $\Gamma_{l_0}(d)$

In accordance with the idea proposed by Miehe et. al. (Miehe et. al. 2010), the potential energy functional  $\Pi$  is given as

$$\Pi(\mathbf{u}, d) = \int_{\Omega} \psi_e(\boldsymbol{\varepsilon}(\mathbf{u})) d\Omega + \int_{\Omega} G_c \left[ \frac{1}{2} l_0 \nabla d \cdot \nabla d + \frac{d^2}{2l_0} \right] d\Omega, \quad (1)$$

where  $\boldsymbol{\varepsilon}$  is the small strain tensor,  $G_c$  is the critical energy release rate,  $\psi_e$  is the elastic strain energy density,  $d$  is a damage or phase field variable, a value between 0



(undamaged) and 1 (fully cracked), and  $l_o$  is the characteristic length to adjust the width of crack diffusion as illustrated in Fig. 1b.

The decomposition of strain tensor proposed by Miehe (Miehe et. al. 2010) is used to prevent non-physical fracture due to compression and only to consider fracture due to tension. The decomposition based on the spectral decomposition is can be written as

$$\boldsymbol{\varepsilon} = \boldsymbol{\varepsilon}_+ + \boldsymbol{\varepsilon}_-, \quad (2)$$

$$\boldsymbol{\varepsilon}_\pm = \sum \langle \varepsilon_a \rangle_\pm \mathbf{n}_a \otimes \mathbf{n}_a, \quad (3)$$

in which  $\boldsymbol{\varepsilon}_+$  and  $\boldsymbol{\varepsilon}_-$  are the positive and negative components of the strain tensor, respectively,  $\varepsilon_a$  is the eigenvalue of the strain tensor,  $\mathbf{n}_a$  is the eigenvector of the strain tensor, and  $\langle \cdot \rangle_\pm$  is the Macaulay bracket operator defined as

$$\langle x \rangle_\pm = \frac{1}{2} x \pm |x|. \quad (4)$$

In addition, the elastic strain energy density function is also divided into the positive and negative parts

$$\psi_e = g(d)\psi_e^+(\boldsymbol{\varepsilon}) + \psi_e^-(\boldsymbol{\varepsilon}), \quad (5)$$

$$\psi_e^\pm(\boldsymbol{\varepsilon}) = \frac{1}{2} \lambda \langle \text{tr}(\boldsymbol{\varepsilon}) \rangle_\pm^2 + \mu \text{tr}[\boldsymbol{\varepsilon}_\pm^2], \quad (6)$$

$$g(d) = [(1-d)^2 + k], \quad (7)$$

where  $\psi_e^+$  and  $\psi_e^-$  are the positive and negative parts of the elastic strain energy density function,  $g(d)$  is a degradation function to handle stress degradation.  $k$  is a very small parameter to avoid numerical singularities.

## 2.2. Governing equations

The strong form of governing equations is expressed as

$$\nabla \cdot \boldsymbol{\sigma} + \mathbf{b} = 0, \quad (8)$$

$$\left[ \frac{G_c}{l_o} + 2\psi_e^+ \right] d - G_c l_o \nabla d \cdot \nabla d = 2\psi_e^+, \quad (9)$$



where  $\mathbf{b}$  is the body force. Note that Eq. (8) and Eq. (9) are obtained by performing the variation operations on Eq. (1).

In order to account for the irreversibility of crack growth, the local history field is introduced as

$$H(x,t) = \max_{s \in [0,t]} \psi_e^+(\boldsymbol{\varepsilon}(\mathbf{x},s)), \quad (10)$$

where  $H(x,t)$  is the local history field, which replaces the elastic strain energy density function  $\psi_e^+$ .

### 3. Adaptive mesh refinement strategy

We define the radius of the crack tip area as  $r_c$ , and use fine meshes within the radius  $r_c$  and coarse meshes outside the radius  $r_c$  shown in Fig. 2a and Fig. 2b. Using variable-node finite elements (Lim et. al. 2012) illustrated in Fig 2c, the fine mesh and the coarse mesh are connected as described in Fig 2b.

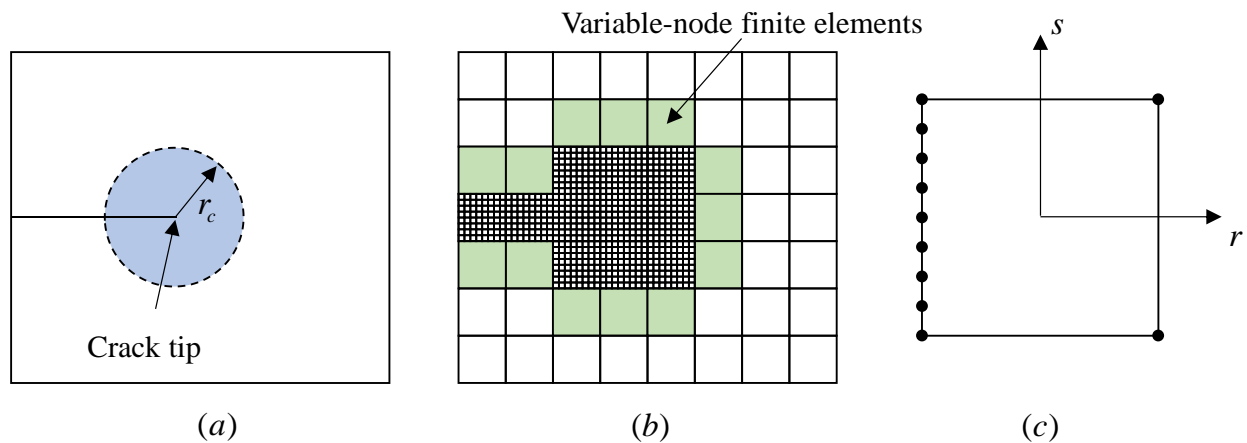


Fig. 2 (a) Domain around the crack tip (b) Mesh geometry for the adaptive refinement strategy (c) Variable-node finite element in the natural coordinate system

### 4. Numerical example: Single-edge notched tension test

A square plate with a single-edge crack is considered as shown in Fig. 3a. All dimensions are in mm. A prescribed vertical displacement is applied to the top edge of the plate. The material properties of this plate are given by  $E = 210$  GPa,  $\nu = 0.3$  and  $G_c = 2.7 \times 10^{-3}$  kN/mm. The characteristic length is taken as  $l_o = 0.0075$  mm. The mesh geometry for the local refinement strategy (21791 elements) and for the adaptive refinement strategy (50x50 elements) are considered as illustrated in Fig. 3b and Fig. 3c, respectively. For the initial 500 load steps,  $\Delta u_y = 1 \times 10^{-5}$  mm is prescribed, after that



$\Delta u_y = 1 \times 10^{-6}$  mm is prescribed for 1300 load steps. The mesh geometry and crack pattern for the adaptive refinement strategy during crack propagation are described in Fig. 4. The load-displacement curve is illustrated in Fig. 5. The computation time is shown in Table 1. From Fig. 5 and Table 1, we can confirm that the computational performance and efficiency of the adaptive refinement strategy is excellent compared with those of the local refinement strategy.

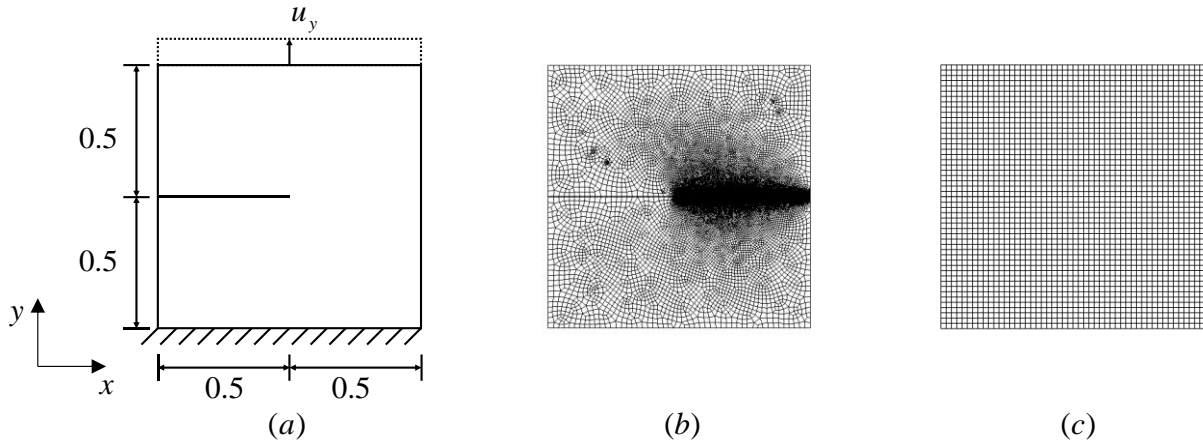


**Fig. 3** (a) Geometry and boundary conditions for the single-edge notched tension test, (b) Mesh geometry for the local refinement strategy, (c) Initial mesh geometry for the adaptive refinement strategy

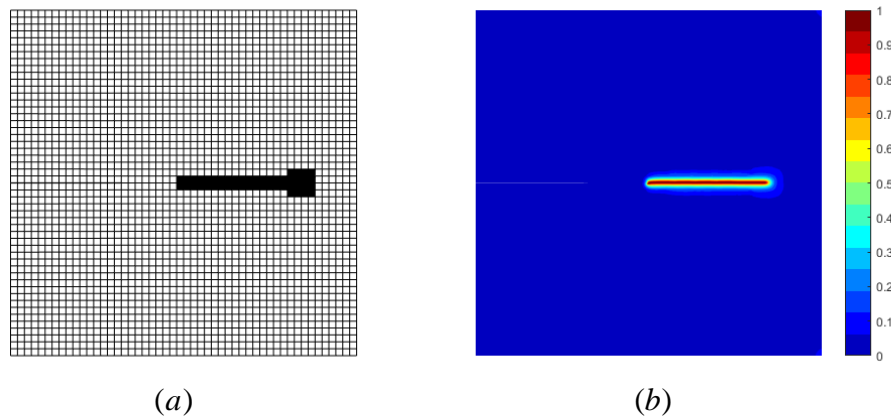


**Fig. 4** (a) Mesh geometry for the adaptive refinement strategy during crack propagation, (b) Crack pattern for the adaptive refinement strategy

## 5. CONCLUSIONS

In this study, an adaptive mesh refinement strategy for the phase field method to simulate brittle fracture problems was presented. The performance of the adaptive mesh refinement strategy was compared with those of the local mesh refinement strategy through a two-dimensional crack numerical example. As a result, it was shown that the



adaptive mesh refinement strategy has excellent computational efficiency while maintaining accuracy. In the future, we will extend this study by applying numerical techniques such as the strain smoothing method (Lee et. al. 2018) and the enriched finite element (Kim et. al. 2018, Kim et. al. 2019). Furthermore, it is valuable to extend this study to shell fractures (Lee et. al. 2014, Jeon et. al. 2015, Lee et. al. 2015, Ko et. al. 2016, Ko et. al. 2017, Ko et. al. 2017, Ko et. al. 2017, Jun et. al. 2018, Lee et. al. 2019).

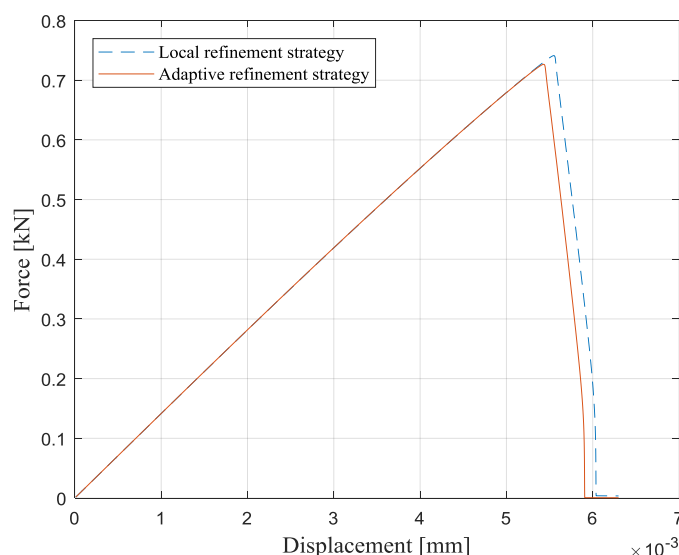


**Fig. 5** Load-displacement curve of single-edge notched tension test

**Table 1** Computation time for the single-edge notched tension test

	Computation time	
	[sec]	Ratio [%]
Local refinement strategy	49989.34	100.00
Adaptive refinement strategy	5466.08	10.93

## REFERENCES

- Miehe, C., Hofacker, M., Welschinger, F. (2010), "A phase field model for rate-independent crack propagation: Robust algorithmic implementation based on operator splits", *Computer Methods in Applied Mechanics and Engineering*, **199**(45-48), 2765-2778.
- Patil, R. U., Mishra, B. K., Singh, I. V. (2018), "An adaptive multiscale phase field method for brittle fracture", *Computer Methods in Applied Mechanics and Engineering*, **329**, 254-288.
- Tian, F., Tang, X., Xu, T., Yang, J., Li, L. (2019), "A hybrid adaptive finite element phase-field method for quasi-static and dynamic brittle fracture", *International Journal for Numerical Methods in Engineering*, **120**(9), 1108-1125.

*The 2020 World Congress on  
The 2020 Structures Congress (Structures20)  
25-28, August, 2020, GECE, Seoul, Korea*



- Lim, J. H., Sohn, D., Im, S. (2012), "Variable-node element families for mesh connection and adaptive mesh computation", *Structural Engineering and Mechanics*, **43**(3), 349-370.
- Lee, C., Lee, P. S. (2018), "A new strain smoothing method for triangular and tetrahedral finite elements", *Computer Methods in Applied Mechanics and Engineering*, **341**, 939-955.
- Kim, S., Lee, P. S. (2018), "A new enriched 4-node 2D solid finite element free from the linear dependence problem", *Computers & Structures*, **202**, 25-43.
- Kim, S., Lee, P. S. (2019), "New enriched 3D solid finite elements: 8-node hexahedral, 6-node prismatic, and 5-node pyramidal elements", *Computers & Structures*, **216**, 40-63.
- Lee, Y., Lee, P. S., Bathe, K. J. (2014), "The MITC3+ shell element and its performance", *Computers & Structures*, **138**, 12-23.
- Jeon, H. M., Lee, Y., Lee, P. S., Bathe, K. J. (2015), "The MITC3+ shell element in geometric nonlinear analysis", *Computers & Structures*, **146**, 91-104.
- Lee, Y., Jeon, H. M., Lee, P. S., Bathe, K. J. (2015), "The modal behavior of the MITC3+ triangular shell element", *Computers & Structures*, **153**, 148-164.
- Ko, Y., Lee, P. S., Bathe, K. J. (2016), "The MITC4+ shell element and its performance", *Computers & Structures*, **169**, 57-68.
- Ko, Y., Lee, P. S., Bathe, K. J. (2017), "A new MITC4+ shell element", *Computers & Structures*, **182**, 404-418.
- Ko, Y., Lee, P. S., Bathe, K. J. (2017), "The MITC4+ shell element in geometric nonlinear analysis", *Computers & Structures*, **185**, 1-14.
- Ko, Y., Lee, P. S., Bathe, K. J. (2017), "A new 4-node MITC element for analysis of two-dimensional solids and its formulation in a shell element", *Computers & Structures*, **192**, 34-49.
- Jun, H., Yoon, K., Lee, P. S., Bathe, K. J. (2018), "The MITC3+ shell element enriched in membrane displacements by interpolation covers", *Computer Methods in Applied Mechanics and Engineering*, **337**, 458-480.
- Lee, C., Lee, P. S. (2019), "The strain-smoothed MITC3+ shell finite element", *Computers & Structures*, **223**, 106096.
- Inglis, C. E. (1913), "Stresses in a plate due to the presence of cracks and sharp corners", *Trans Inst Naval Archit*, **55**, 219-241.
- Griffith, A. A. (1921), "VI. The phenomena of rupture and flow in solids", *Philosophical transactions of the royal society of london. Series A, containing papers of a mathematical or physical character*, **221**(582-593), 163-198.
- Belytschko, T., Black, T. (1999), "Elastic crack growth in finite elements with minimal remeshing", *International journal for numerical methods in engineering*, **45**(5), 601-620.
- Silling, S. A. (2000), "Reformulation of elasticity theory for discontinuities and long-range forces", *Journal of the Mechanics and Physics of Solids*, **48**(1), 175-209.
- Francfort, G. A., Marigo, J. J. (1998), "Revisiting brittle fracture as an energy minimization problem", *Journal of the Mechanics and Physics of Solids*, **46**(8), 1319-1342.